Multiscale Representations of Manifold-Valued Curves via Subdivision Schemes

Wael Mattar

September 2022

A joint work with Nir Sharon

TEL AVIV UNIVERSITY אוניברסיטת תל אביב

Outline

Outline

Curves on manifolds

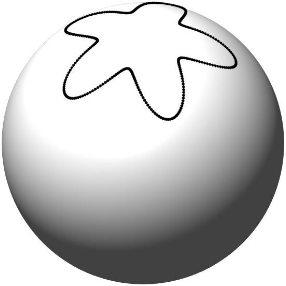

A trajectory on the sphere $S^2 \subset \mathbb{R}^3$.

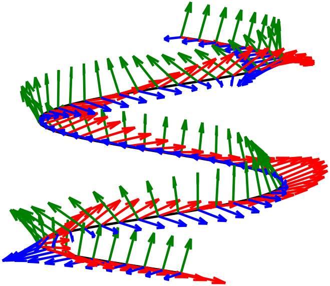

Visualization of a trajectory in the special Euclidean group.

Subdivision schemes

Main idea: define the desired object via **local** refinement,

$$\mathcal{P}^0 \Rightarrow \mathcal{P}^1 \Rightarrow \mathcal{P}^2 \Rightarrow \mathcal{P}^3 \dots \mathcal{P}^\infty$$

Subdivision schemes

Main idea: define the desired object via **local** refinement,

$$\mathcal{P}^0 \Rightarrow \mathcal{P}^1 \Rightarrow \mathcal{P}^2 \Rightarrow \mathcal{P}^3 \cdots \mathcal{P}^\infty$$

For example,

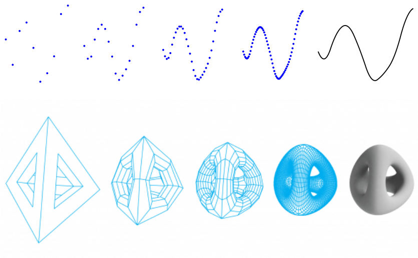

Multiscale representation

Analysis: decomposing an $\mathcal{M}$-valued sequence $\boldsymbol{c}^{(J)}$, associated with scale $J \in \mathbb{N}$, to $\{\boldsymbol{c}^{(0)}; \boldsymbol{d}^{(1)}, \boldsymbol{d}^{(2)}, \ldots, \boldsymbol{d}^{(J)}\}$.
Synthesis: recover $\boldsymbol{c}^{(J)}$ from an $\mathcal{M}$-valued coarse approximation of resolution 0, $\boldsymbol{c}^{(0)}$, using the detail coefficients $\boldsymbol{d}^{(\ell)}$ of scale $\ell = 1, 2, \ldots, J$.

Multiscale representation

Analysis: decomposing an $\mathcal{M}$-valued sequence $\boldsymbol{c}^{(J)}$, associated with scale $J \in \mathbb{N}$, to $\{\boldsymbol{c}^{(0)}; \boldsymbol{d}^{(1)}, \boldsymbol{d}^{(2)}, \ldots, \boldsymbol{d}^{(J)}\}$.

Synthesis: recover $\boldsymbol{c}^{(J)}$ from an $\mathcal{M}$-valued coarse approximation of resolution 0, $\boldsymbol{c}^{(0)}$, using the detail coefficients $\boldsymbol{d}^{(\ell)}$ of scale $\ell = 1, 2, \ldots, J$.

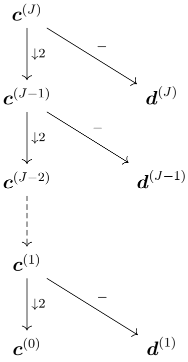

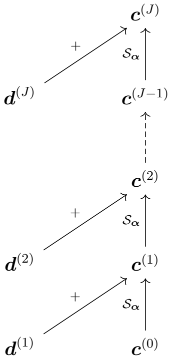

Outline

Interpolating subdivision scheme & pyramid transform

- Interpolating subdivision scheme operator $\mathcal{S}_{\boldsymbol{\alpha}}$ satisfies

$$(\mathcal{S}_{\boldsymbol{\alpha}}\boldsymbol{c})_{2k} = \boldsymbol{c}_k, \quad k \in \mathbb{Z}.$$

Interpolating subdivision scheme & pyramid transform

- Interpolating subdivision scheme operator $\mathcal{S}_\alpha$ satisfies

$$(\mathcal{S}_\alpha \boldsymbol{c})_{2k} = \boldsymbol{c}_k, \quad k \in \mathbb{Z}.$$

Interpolating decomposition

Given a real-valued sequence $\boldsymbol{c}^{(1)}$, the decomposition is

$$\boldsymbol{c}^{(0)} = \boldsymbol{c}^{(1)} \downarrow 2, \quad \text{and} \quad \boldsymbol{d}^{(1)} = \boldsymbol{c}^{(1)} - \mathcal{S}_\alpha \boldsymbol{c}^{(0)}.$$

Interpolating subdivision scheme & pyramid transform

- Interpolating subdivision scheme operator $\mathcal{S}_\alpha$ satisfies

$$(\mathcal{S}_\alpha \boldsymbol{c})_{2k} = \boldsymbol{c}_k, \quad k \in \mathbb{Z}.$$

Interpolating decomposition

Given a real-valued sequence $\boldsymbol{c}^{(1)}$, the decomposition is

$$\boldsymbol{c}^{(0)} = \boldsymbol{c}^{(1)} \downarrow 2, \quad \text{and} \quad \boldsymbol{d}^{(1)} = \boldsymbol{c}^{(1)} - \mathcal{S}_\alpha \boldsymbol{c}^{(0)}.$$

$\Rightarrow$ Details satisfy $\boldsymbol{d}^{(1)} \downarrow 2 = \mathbf{0}$ which is equivalent to

$$\boxed{[(\mathcal{I} - \mathcal{S}_\alpha \downarrow 2)\boldsymbol{c}^{(1)}] \downarrow 2 = \mathbf{0}}$$

The non-interpolatory case

For non-interpolatory upsampling operator, it is no longer true that $\boldsymbol{d}^{(1)} \downarrow 2 = \mathbf{0}$. Therefore, we need to fill this gap.

The non-interpolatory case

Decimation operator

Let $\mathcal{S}_{\boldsymbol{\alpha}}$ be non-interpolating subdivision operator, we say that $\mathcal{D}_{\boldsymbol{\gamma}}$ is its corresponding even-inverse operator if

$$[(\mathcal{I} - \mathcal{S}_{\boldsymbol{\alpha}} \mathcal{D}_{\boldsymbol{\gamma}}) \boldsymbol{c}] \downarrow 2 = \mathbf{0},$$

where $\mathcal{I}$ is the identity operator.

The non-interpolatory case

Decimation operator

Let $\mathcal{S}_{\alpha}$ be non-interpolating subdivision operator, we say that $\mathcal{D}_{\gamma}$ is its corresponding even-inverse operator if

$$[(\mathcal{I} - \mathcal{S}_{\alpha}\mathcal{D}_{\gamma})\boldsymbol{c}] \downarrow 2 = \mathbf{0},$$

where $\mathcal{I}$ is the identity operator.

- The application of $\mathcal{D}_{\gamma}$ on points $\boldsymbol{c}$ yields to fewer points representing a coarse approximation of $\boldsymbol{c}$.
- The operator $\mathcal{D}_{\gamma}$ is given explicitly via $\boldsymbol{\gamma} * (\boldsymbol{\alpha} \downarrow 2) = \boldsymbol{\delta}$.
- The sequence $\boldsymbol{\gamma}$ is infinitely supported, sums to 1, and is bounded by a geometrically decreasing sequence.

Pyramid transform with decimation

$$\boxed{\text{Sequence } \boldsymbol{c}^{(J)}} \underset{\text{reconstruction}}{\overset{\text{decomposition}}{\rightleftharpoons}} \boxed{\text{Pyramid } \left\{ \boldsymbol{c}^{(0)}; \boldsymbol{d}^{(1)}, \boldsymbol{d}^{(2)}, \ldots, \boldsymbol{d}^{(J)} \right\}}$$

Pyramid transform with decimation

$$\boxed{\text{Sequence } \boldsymbol{c}^{(J)}} \underset{\text{reconstruction}}{\overset{\text{decomposition}}{\rightleftharpoons}} \boxed{\text{Pyramid } \left\{ \boldsymbol{c}^{(0)}; \boldsymbol{d}^{(1)}, \boldsymbol{d}^{(2)}, \ldots, \boldsymbol{d}^{(J)} \right\}}$$

Pyramid transform

Given a real-valued sequence $\boldsymbol{c}^{(J)}$, $J \in \mathbb{N}$, we define the multiscale transform iteratively by

$$\boldsymbol{c}^{(\ell-1)} = \mathcal{D}_\gamma \boldsymbol{c}^{(\ell)}, \quad \boldsymbol{d}^{(\ell)} = \boldsymbol{c}^{(\ell)} - \mathcal{S}_\alpha \boldsymbol{c}^{(\ell-1)}, \quad \ell = J,\ J-1,\ \ldots,\ 1.$$

Pyramid transform with decimation

$$\boxed{\text{Sequence } \boldsymbol{c}^{(J)}} \underset{\text{reconstruction}}{\overset{\text{decomposition}}{\rightleftharpoons}} \boxed{\text{Pyramid } \left\{ \boldsymbol{c}^{(0)}; \boldsymbol{d}^{(1)}, \boldsymbol{d}^{(2)}, \ldots, \boldsymbol{d}^{(J)} \right\}}$$

Pyramid transform

Given a real-valued sequence $\boldsymbol{c}^{(J)}$, $J \in \mathbb{N}$, we define the multiscale transform iteratively by

$$\boldsymbol{c}^{(\ell-1)} = \mathcal{D}_\gamma \boldsymbol{c}^{(\ell)}, \quad \boldsymbol{d}^{(\ell)} = \boldsymbol{c}^{(\ell)} - \mathcal{S}_\alpha \boldsymbol{c}^{(\ell-1)}, \quad \ell = J,\ J-1,\ \ldots,\ 1.$$

Inverse transform

The sequence $\boldsymbol{c}^{(J)}$ can be synthesized iteratively via

$$\boldsymbol{c}^{(\ell)} = \mathcal{S}_\alpha \boldsymbol{c}^{(\ell-1)} + \boldsymbol{d}^{(\ell)}, \quad \ell = 1,\ 2,\ \ldots,\ J.$$

Outline

The linear subdivision rewritten

The linear refinement $(\mathcal{S}_{\boldsymbol{\alpha}}\boldsymbol{c})_k = \sum_{i\in\mathbb{Z}} \alpha_{k-2i} c_i$ can be seen as the unique real solution X of,

$$\sum_{i\in\mathbb{Z}} \alpha_{k-2i}(c_i - X) = 0, \quad k \in \mathbb{Z}.$$

Therefore, we can rewrite the refinement rule as

$$\boxed{(\mathcal{S}_{\boldsymbol{\alpha}}\boldsymbol{c})_k = \mathrm{argmin}_{X\in\mathbb{R}} \sum_{i\in\mathbb{Z}} \alpha_{k-2i}\|c_i - X\|^2, \quad k \in \mathbb{Z}.}$$

The manifold-valued refinement rule

Geodesic distance: Given a Riemannian manifold $(\mathcal{M}, \rho)$ associated with metric,

$$\rho(x, y) := \inf_{\Gamma} \int_a^b |\dot{\Gamma}(t)| dt,$$

where $\Gamma : [a, b] \to \mathcal{M}$ is a curve connecting points $\Gamma(a) = x$ and $\Gamma(b) = y$, and $| \cdot |^2 = \langle \cdot, \cdot \rangle$.

The manifold-valued refinement rule

Geodesic distance: Given a Riemannian manifold $(\mathcal{M}, \rho)$ associated with metric,

$$\rho(x, y) := \inf_{\Gamma} \int_a^b |\dot{\Gamma}(t)| dt,$$

where $\Gamma : [a, b] \to \mathcal{M}$ is a curve connecting points $\Gamma(a) = x$ and $\Gamma(b) = y$, and $|\cdot|^2 = \langle \cdot, \cdot \rangle$.

We define $\mathcal{T}_{\boldsymbol{\alpha}}$ to be the Riemannian counterpart of $\mathcal{S}_{\boldsymbol{\alpha}}$ by using the Riemannian Center of Mass (R-CoM), also known as Karcher or Fréchet means,

$$(\mathcal{T}_{\boldsymbol{\alpha}} \boldsymbol{c})_k := \operatorname{argmin}_{X \in \mathcal{M}} \sum_{i \in \mathbb{Z}} \alpha_{k-2i} \rho^2(c_i, X), \quad k \in \mathbb{Z}.$$

Manifold-valued operators for the multiscale

The corresponding decimation operator $\mathcal{Y}_\zeta$ can be extended to $\mathcal{M}$ in a similar way, based on the R-CoM and the linear schemes.

Manifold-valued operators for the multiscale

The corresponding decimation operator $\mathcal{Y}_\zeta$ can be extended to $\mathcal{M}$ in a similar way, based on the R-CoM and the linear schemes.

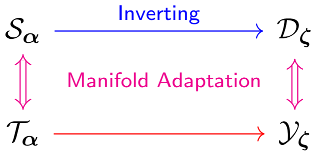

Multiscale transform on manifolds

Denote the exponential map of a vector v in the tangent space $T_b\mathcal{M}$ around a base point b and its inverse logarithm map by

$$b \oplus v = \mathrm{Exp}_b(v), \quad \text{and} \quad q \ominus b = \mathrm{Log}_b(q), \quad b, q \in \mathcal{M}\,.$$

Multiscale transform on manifolds

Denote the exponential map of a vector v in the tangent space $T_b\mathcal{M}$ around a base point b and its inverse logarithm map by

$$b \oplus v = \operatorname{Exp}_b(v), \quad \text{and} \quad q \ominus b = \operatorname{Log}_b(q), \quad b, q \in \mathcal{M}\,.$$

Pyramid transform for manifold values

Given a $\mathcal{M}$-valued sequence $\boldsymbol{c}^{(J)}$, $J \in \mathbb{N}$, we define the multiscale transform iteratively by

$$\boldsymbol{c}^{(\ell-1)} = \mathcal{Y}_\zeta \boldsymbol{c}^{(\ell)}, \quad \boldsymbol{d}^{(\ell)} = \boldsymbol{c}^{(\ell)} \ominus \mathcal{T}_\alpha \boldsymbol{c}^{(\ell-1)}, \quad \ell = J,\ J-1,\ \ldots,\ 1.$$

Note that the detail coefficients live in the tangent bundle $T\mathcal{M}$.

Multiscale transform on manifolds

Denote the exponential map of a vector v in the tangent space $T_b\mathcal{M}$ around a base point b and its inverse logarithm map by

$$b \oplus v = \operatorname{Exp}_b(v), \quad \text{and} \quad q \ominus b = \operatorname{Log}_b(q), \quad b, q \in \mathcal{M}.$$

Pyramid transform for manifold values

Given a $\mathcal{M}$-valued sequence $\boldsymbol{c}^{(J)}$, $J \in \mathbb{N}$, we define the multiscale transform iteratively by

$$\boldsymbol{c}^{(\ell-1)} = \mathcal{Y}_\zeta \boldsymbol{c}^{(\ell)}, \quad \boldsymbol{d}^{(\ell)} = \boldsymbol{c}^{(\ell)} \ominus \mathcal{T}_\alpha \boldsymbol{c}^{(\ell-1)}, \quad \ell = J,\ J-1,\ \ldots,\ 1.$$

Note that the detail coefficients live in the tangent bundle $T\mathcal{M}$.

Inverse transform

The sequence $\boldsymbol{c}^{(J)}$ can be synthesized iteratively via

$$\boldsymbol{c}^{(\ell)} = \mathcal{T}_\alpha \boldsymbol{c}^{(\ell-1)} \oplus \boldsymbol{d}^{(\ell)}, \quad \ell = 1, 2, \ldots, J.$$

Analytical results

What properties does the pyramid transform satisfy?

Analytical results

Corollary (coefficients decay)

If the sequence $\boldsymbol{c}^{(J)}$ is sampled from a differentiable $\mathcal{M}$-valued curve f over an arc-length equidistanced grid with scale J. Then,

$$\|\boldsymbol{d}^{(\ell)}\|_\infty \leq KP^J \sup_t \|\nabla f(t)\| \cdot (2P)^{-\ell}, \quad \ell = 1, 2, \ldots, J,$$

for some $P > 1$ and $K \geq 0$ depending on the curvature of $\mathcal{M}$.

Analytical results

Theorem (stability)

Let $\mathcal{M}$ be a complete, open manifold with non-negative sectional curvature. Let $\{\boldsymbol{c}^{(0)}; \boldsymbol{d}^{(1)}, \dots, \boldsymbol{d}^{(J)}\}$ and $\{\widetilde{\boldsymbol{c}}^{(0)}; \widetilde{\boldsymbol{d}}^{(1)}, \dots, \widetilde{\boldsymbol{d}}^{(J)}\}$ be two pyramids. Then the synthesis sequences $\boldsymbol{c}^{(J)}$ and $\widetilde{\boldsymbol{c}}^{(J)}$ satisfy

$$\mu(\boldsymbol{c}^{(J)}, \widetilde{\boldsymbol{c}}^{(J)}) \leq L\left(\mu(\boldsymbol{c}^{(0)}, \widetilde{\boldsymbol{c}}^{(0)}) + \sum_{i=1}^{J} \|\widehat{\boldsymbol{d}}^{(i)} - \widetilde{\boldsymbol{d}}^{(i)}\|_\infty\right)$$

where $\widehat{\boldsymbol{d}}^{(i)}$ is the parallel transport of $\boldsymbol{d}^{(i)}$ along the geodesics connecting $\boldsymbol{c}^{(i)}$ with $\mathcal{T}_\alpha \widetilde{\boldsymbol{c}}^{(i-1)}$, element-wise, and $\mu(\boldsymbol{c}, \widetilde{\boldsymbol{c}}) = \sup_{k \in \mathbb{Z}} \rho(c_k, \widetilde{c}_k)$.

Outline

Representing a curve on the sphere

We consider the pyramid transform using the cubic B-spline scheme.

Representing a curve on the sphere

We consider the pyramid transform using the cubic B-spline scheme.

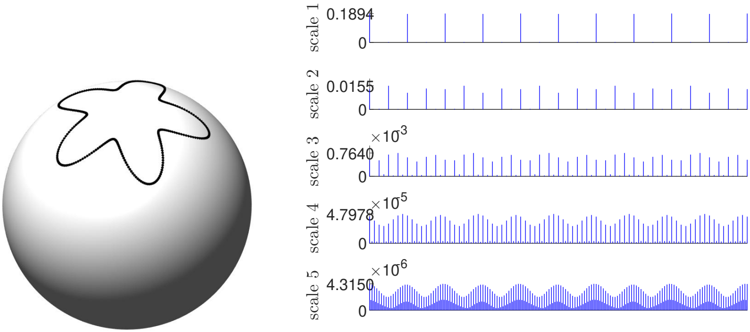

A smooth $\mathbb{S}^2$-valued curve with its corresponding multiscale representation. Decay of detail coefficients indicate the smoothness of the curve.

Denoising the curve over the sphere

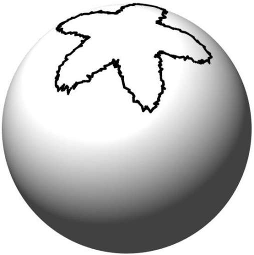

Denoising the curve over the sphere

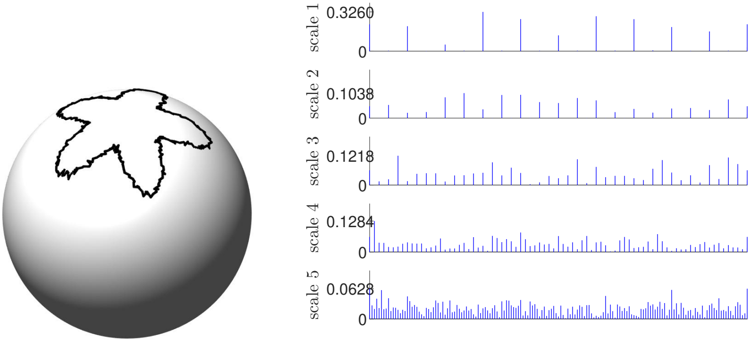

The curve contaminated with noise points and the corresponding representation. Large norms on high scales indicating non-smoothness.

Denoising the curve over the sphere (cont.)

Denoising via thresholding: we set to zero all detail coefficients with norm below a fixed threshold. We synthesized the resulted sparse representation.

Denoising the curve over the sphere (cont.)

Denoising via thresholding: we set to zero all detail coefficients with norm below a fixed threshold. We synthesized the resulted sparse representation.

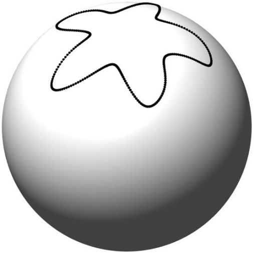

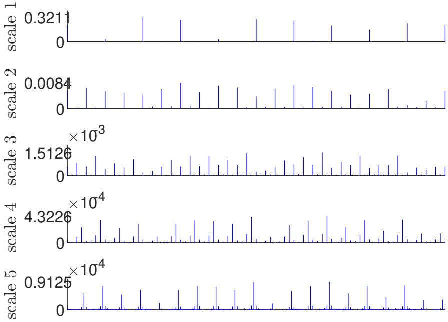

Anomaly Detection in a time series over $\mathcal{SPD}(3)$

Let $\mathcal{M} = \mathcal{SPD}(3)$ be the cone of symmetric positive definite matrices.

Anomaly Detection in a time series over $\mathcal{SPD}(3)$

Let $\mathcal{M} = \mathcal{SPD}(3)$ be the cone of symmetric positive definite matrices.

The $\mathcal{SPD}$ matrices are visualized by centric ellipsoids:

The first $\mathcal{SPD}(3)$-valued sequence

The second $\mathcal{SPD}(3)$-valued sequence – with two "jump" points

Anomaly Detection over $\mathcal{SPD}(3)$

We apply the pyramid transform based upon the corner-cutting scheme.

Anomaly Detection over $\mathcal{SPD}(3)$

We apply the pyramid transform based upon the corner-cutting scheme.

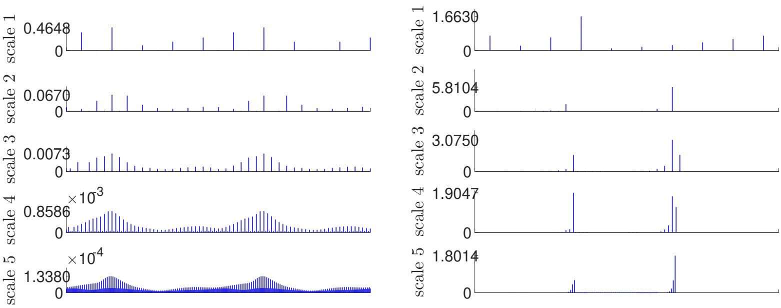

Frobenius norms of the details coefficients. On the left, the multiscale representation of the first (smooth) sequence. On the right, the representation of the second sequence. The jump locations are clearly seen via the large magnitude detail coefficients.

Contrast Enhancement over SO(3)

We apply the pyramid transform based upon least squares scheme.

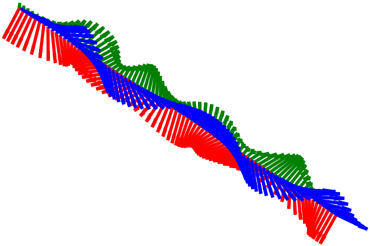

Contrast Enhancement over SO(3)

We apply the pyramid transform based upon least squares scheme.

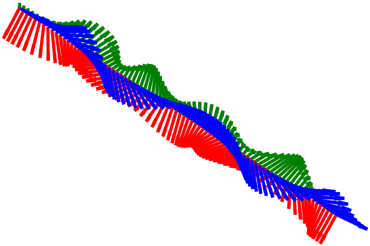

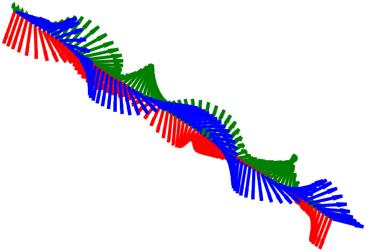

On the left, the raw trajectory of rotation matrices. On the right, the result of contrast-enhancing the trajectory. The detail coefficients were enlarged by 50%. The drastic deflections exhibit the effect of the application.

Thanks for your attention!
Questions?